Possible new phenomenology in turbostratic graphene bilayer as a solid-state realization of a two-brane universe model

Michaël Sarrazin[1,*] and Fabrice Petit[2,†]

[1]*Research Center in Physics of Matter and Radiation (PMR), Department of Physics, University of Namur (FUNDP), 61 rue de Bruxelles, B-5000 Namur, Belgium*
[2]*BCRC (Member of EMRA), 4 avenue du gouverneur Cornez, B-7000 Mons, Belgium*

It is suggested that two turbostratic graphene layers can be described through a formalism previously introduced for the study of braneworlds in high energy physics. It is demonstrated that any graphene bilayer can be conveniently described as a "noncommutative" two-sheeted (2+1) spacetime. The model Hamiltonian contains a coupling term connecting the two layers which is a reminiscent of the coupling which may exist between two braneworlds at a quantum level. In the present case, this term is related to a $K-K'$ intervalley coupling. Phenomenological consequences are emphasized such as exciton swapping between the two graphene sheets. An experimental device is suggested to study this possible new effect. If demonstrated, this effect could be an indirect way to test some theoretical concepts of the braneworld hypothesis. Technological applications are underlined.

PACS numbers: 72.80.Vp, 78.67.Wj, 11.25.Wx, 02.40.Gh

I. INTRODUCTION

During the last few years, graphene has taken a growing importance in solid states physics [1–22]. Indeed, it is an amazing case of two-dimensional carbon crystal, and its remarkable properties make it a strategic material for future nanotechnologies. From a fundamental and theoretical point of view, graphene is also a solid-state realization of a $(2+1)$ spacetime in which massless fermions live. Thus, graphene is a remarkable tool to experiment some theoretical concepts of low-dimensional electrodynamics and quantum dynamics [11–15]. Graphene could be also an efficient tool to test some theoretical ideas taking their origins in high energy physics. During the last two decades, the possibility that our observable $(3+1)$-dimensional Universe could be a sheet (a $3-$brane or braneworld) embedded in a $(N+1)$-dimensional spacetime (called the bulk, with $N>3$) has received a lot of attention [23]. Such an exotic concept appears very productive to solve puzzling problems beyond the standard model of particles [23]. Nevertheless, braneworld models remain complex especially to confront theoretical solutions with experiments. However, in recent papers, a mathematical and physical tool was introduced to simplify the study of a universe made of two branes [24–27]. At low energies, the quantum dynamics of Dirac fermions in such a two-world can be rigorously described by a more simple and equivalent model that corresponds to a two-sheeted spacetime in the formalism of the noncommutative geometry [24, 25]. The model reveals a coupling term in the Hamiltonian which connects the two branes: Particles endowed with a magnetic moment undergo Rabi oscillations between those worlds under the influence of a magnetic vector potential [24–27].

On another hand, recent works on graphene underline the importance of electronic transport in turbostratic bilayers [3–9]. Since a graphene sheet can be considered as $2-$brane embedded in a $(3+1)$ bulk, a graphene bilayer could be a solid-state realization of a universe containing two branes (a two-brane universe). In the present paper, we show that this analogy is well-sounded and demonstrate the possibility to apply our noncommutative geometry tool to study a graphene bilayer. This approach suggests that exciton swapping may occur between the two layers. Thus a possible new experimental phenomenon would be a solid-state counterpart of the particle oscillations predicted in brane theory [24–27].

In section II, we recall the basic assumptions underlying the description of electron and hole in graphene through a Dirac equation formalism. Next, in section III, we present our model of fermion dynamics in a two-sheeted spacetime and its adaptation to describe a set of two graphene layers. Then, in section IV, using a tight-binding approach, we show that two turbostratic graphene layers are a prerequisite to get a $K-K'$ intervalley coupling between two perfect graphene layers in mutual interaction. This coupling may result in exciton swapping between the two layers as shown in section V. Finally, in section VI, an experimental device is suggested to investigate this new effect.

II. GRAPHENE ELECTRONIC PROPERTIES

Graphene is a one-atom thick layer made of sp^2 carbon atoms in an hexagonal lattice arrangement (Fig.1a) [1, 2]. Self-supported ideal graphene is a zero-gap semiconductor. In the vicinity of the six corners (called Dirac points) of the two-dimensional hexagonal Brillouin zone (Fig.1b), the electronic dispersion relation is linear for low energies (Fig.1c). Electrons (and holes) can then

*Electronic address: michael.sarrazin@fundp.ac.be
†Electronic address: f.petit@bcrc.be

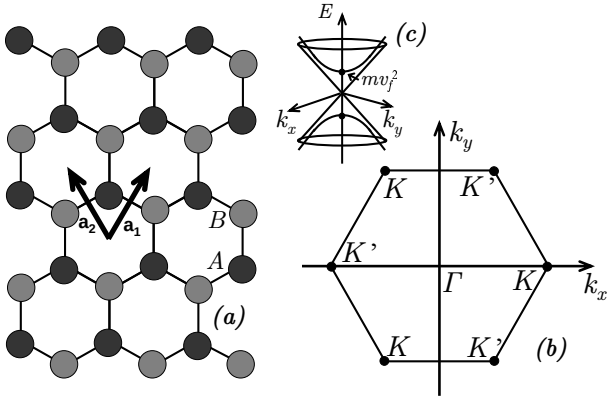

FIG. 1: (a) Hexagonal lattice of graphene with the two sublattices A and B. a_1 and a_2 are the vectors of the unit cell. (b) Brillouin zone of the hexagonal lattice. (c) Energy behavior in the vicinity of the Dirac points K and K'.

be described by a Dirac equation for massless spin$-1/2$ particles in an effective $(2+1)$ spacetime [2]. While massless Dirac fermions propagate at the speed of light in the $(3+1)$ Minkowski spacetime, in graphene the effective massless Dirac fermions propagates at the Fermi velocity ($v_F \approx 10^6$ m$\cdot$s^{-1} in the present case). On a graphene layer, the Hamiltonian of the effective Dirac equation is given by [2]:

$$H_{\pm} = -i\hbar v_F(\sigma_1\partial_x \pm \sigma_2\partial_y) + mv_f^2\sigma_3 \qquad (1)$$

where "+" (respectively "$-$") refers to the K (respectively K') point of the Brillouin zone of the graphene hexagonal structure (Fig.1a). σ_k $(k = 1, 2, 3)$ are the usual Pauli matrices. For a self-supported graphene sheet the mass term m is equal to zero and electrons (and holes) behave as relativistic quasiparticles. Nevertheless m may differ from zero in the case of a sheet deposited on a substrate [16]. Using $m \to mv_F/\hbar$ and $(x_0, x_1, x_2) = (v_F\, t, x, y)$, from Eq. (1) it is possible to conveniently describe the electron (or hole) dynamics through an effective Dirac equation such that [2]:

$$(i\gamma^\eta\partial_\eta - m)\psi = 0 \qquad (2)$$

with $\eta = 0, 1, 2$ and

$$\gamma^0 = \begin{pmatrix} \sigma_3 & 0 \\ 0 & \sigma_3 \end{pmatrix},\ \gamma^1 = \begin{pmatrix} i\sigma_2 & 0 \\ 0 & i\sigma_2 \end{pmatrix},\ \gamma^2 = \begin{pmatrix} -i\sigma_1 & 0 \\ 0 & i\sigma_1 \end{pmatrix} \qquad (3)$$

such that $\{\gamma^\eta, \gamma^\vartheta\} = 2g^{\eta\vartheta}$ $(\eta, \vartheta = 0, 1, 2)$ with $g^{\eta\vartheta}$ =diag$(1, -1, -1)$. The wave function is defined as $\psi = \begin{pmatrix} \chi \\ \theta \end{pmatrix}$ where χ (respectively θ) is related to the wave function on K (respectively K'). In addition, χ (respectively θ) can be written as $\chi = \begin{pmatrix} \chi_A \\ \chi_B \end{pmatrix}$ (respectively $\theta = \begin{pmatrix} \theta_A \\ \theta_B \end{pmatrix}$) where A and B are related to the two sublattices of the graphene sheet (see fig.1a).

It can be noticed that the above $(2+1)$-Dirac equation can be easily extended to its $(3+1)$-dimensional version. γ^3 and γ^5 matrices (such as $\gamma^5 = i\gamma^0\gamma^1\gamma^2\gamma^3$) can be introduced and we may consider for instance:

$$\gamma^3 = \begin{pmatrix} 0 & -\sigma_1 \\ \sigma_1 & 0 \end{pmatrix},\ -i\gamma^5 = \begin{pmatrix} 0 & i\sigma_1 \\ i\sigma_1 & 0 \end{pmatrix} \qquad (4)$$

The Clifford algebra is verified since $\{\gamma^\mu, \gamma^\nu\} = 2g^{\mu\nu}$, $\{\gamma^5, \gamma^\nu\} = 0$ and $(-i\gamma^5)^2 = -\mathbf{1}$, where $g^{\mu\nu}$ is the four-dimensional metric tensor of the Minkowski spacetime $(\mu, \nu = 0, 1, 2, 3)$. Note that the γ^3 and γ^5 matrices are interchangeable through substitutions $\gamma^3 \to i\gamma^5$ and $-i\gamma^5 \to \gamma^3$ which lead to equivalent descriptions. Moreover, it is well known that γ^5 can be also used to define a five-dimensional Dirac equation as shown in section III.

III. TWO-LAYER GRAPHENE AS A "NONCOMMUTATIVE" TWO-SHEETED SPACETIME

Let us consider a graphene layer as a 3-brane, i.e. a three-dimensional space sheet, for which one dimension (say x_3) is reduced to zero. We suggest to derive the graphene bilayer system description from the two-sheeted spacetime model introduced in previous works [24–27] by making $x_3 \to 0$.

In a prior work, the relevance of the two-sheeted approach was rigorously demonstrated for braneworlds described by domain walls [24]. Indeed, when one studies the low-energy dynamics of a spin$-1/2$ particle in a two-brane Universe, the quantum dynamics of this particle is equivalent to the behavior it would have in a two-sheeted spacetime described by noncommutative geometry [24].

Specifically, a two-sheeted spacetime corresponds to the product of a four-dimensional continuous manifold with a discrete two-point space and can be seen as a five-dimensional universe with a fifth dimension reduced to two points with coordinates $\pm\delta/2$. Both sheets are separated by a phenomenological distance δ, which is not the real distance between the graphene layers as shown in the next section. Mathematically, the model relies on a bi-euclidean space $X = M_4 \times Z_2$ in which any smooth function belongs to the algebra $A = C^\infty(M) \oplus C^\infty(M)$ and can be adequately represented by a 2×2 diagonal matrix F =diag(f_1, f_2). In the noncommutative geometry formalism, the expression of the exterior derivative $D = d + Q$, where d acts on M_4 and Q on the Z_2 internal variable, has been given by Connes [28]: $D : (f_1, f_2) \to (df_1, df_2, g(f_2 - f_1), g(f_1 - f_2))$ with $g = 1/\delta$. Viet and Wali [29] have proposed a representation of D acting as a derivative operator and fulfilling the above requirements. Due to the specific geometrical structure of the bulk, this operator is given by:

$$D_\mu = \begin{pmatrix} \partial_\mu & 0 \\ 0 & \partial_\mu \end{pmatrix},\ \mu = 0,1,2,3 \text{ and } D_5 = \begin{pmatrix} 0 & g \\ -g & 0 \end{pmatrix} \tag{5}$$

where the term g acts as a finite difference operator along the discrete dimension. Using (5), one can build the Dirac operator defined as $\not{D} = \Gamma^N D_N = \Gamma^\mu D_\mu + \Gamma^5 D_5$. It is then convenient to consider the following extension of the gamma matrices (by using the Hilbert space of spinors [28]):

$$\Gamma^\mu = \begin{pmatrix} \gamma^\mu & 0 \\ 0 & \gamma^\mu \end{pmatrix} \text{ and } \Gamma^5 = \begin{pmatrix} \gamma^5 & 0 \\ 0 & -\gamma^5 \end{pmatrix} \tag{6}$$

In the present work, γ^μ and $\gamma^5 = i\gamma^0\gamma^1\gamma^2\gamma^3$ are the Dirac matrices defined by relations (3) and (4) relevant for graphene. We can therefore introduce a mass term $M = m\mathbf{1}_{8\times 8}$ as in the standard Dirac equation. The two-sheeted Dirac equation then writes [24–26]:

$$\begin{aligned} \not{D}_{dirac}\Psi &= \left(i\not{D} - M\right)\Psi = \left(i\Gamma^N D_N - M\right)\Psi = \\ &= \begin{pmatrix} i\gamma^\mu\partial_\mu - m & ig\gamma^5 \\ ig\gamma^5 & i\gamma^\mu\partial_\mu - m \end{pmatrix}\begin{pmatrix} \psi_\alpha \\ \psi_\beta \end{pmatrix} = 0 \end{aligned} \tag{7}$$

with $\Psi = \begin{pmatrix} \psi_\alpha \\ \psi_\beta \end{pmatrix}$ the two-sheeted wave function. In this notation, the indices "α" and "β" discriminate each sheet [24–26], i.e. each graphene layer when $x_3 \to 0$. Each component of the wave function ψ is then the probability amplitude of the electron (or hole) in each graphene sheet. It is important to point out the Lagrangian term:

$$\mathcal{L}_c = \overline{\Psi} i\Gamma^5 D_5 \Psi \tag{8}$$

which ensures the coupling between each graphene layer through $K-K'$ processes as explained in section IV. This $\mathcal{L}_c$ term is the main reason for this paper as it allows particle swapping between the graphene layers.

Let us now introduce the effect of an electromagnetic field, i.e. an $U(1)$ gauge field. To be consistent with the two-sheeted structure of the Dirac field Ψ in Eq. (7), the usual $U(1)$ electromagnetic gauge field should be replaced by an extended $U(1)\otimes U(1)$ gauge field [24–26]. Nevertheless, in the present work, we assume that electromagnetic field sources are out of the graphene layers. The group representation $G = diag(\exp(-iq\Lambda_\alpha), \exp(-iq\Lambda_\beta))$ is therefore reduced to $G = diag(\exp(-iq\Lambda), \exp(-iq\Lambda))$. We are looking for an appropriate gauge field such that the covariant derivative becomes $\not{D}_A \to \not{D} + \not{A}$ with the gauge transformation rule $\not{A}' = G\not{A}G^\dagger - iG\left[\not{D}_{dirac}, G^\dagger\right]$. A convenient choice is [24–26]

$$\not{A} = \begin{pmatrix} iq\gamma^\mu A_\mu^\alpha & 0 \\ 0 & iq\gamma^\mu A_\mu^\beta \end{pmatrix} \tag{9}$$

A_μ^α (respectively A_μ^β) is the magnetic vector potential A_μ on the graphene layer α (respectively β). According to the appropriate covariant derivative, the introduction of the gauge field in Eq. (7) leads to [24–26]

$$\begin{pmatrix} i\gamma^\mu(\partial_\mu + iqA_\mu^\alpha) - m & ig\gamma^5 \\ ig\gamma^5 & i\gamma^\mu(\partial_\mu + iqA_\mu^\beta) - m \end{pmatrix}\begin{pmatrix} \psi_\alpha \\ \psi_\beta \end{pmatrix} = 0 \tag{10}$$

Of course, for graphene sheets, we have $x_3 = 0$ which corresponds to two bidimensional sheets instead of three-dimensional space sheets. In addition, we will assume that the experiment under consideration hereafter (section VI) is such that A_μ is parallel to each graphene sheet ($A_3 = 0$).

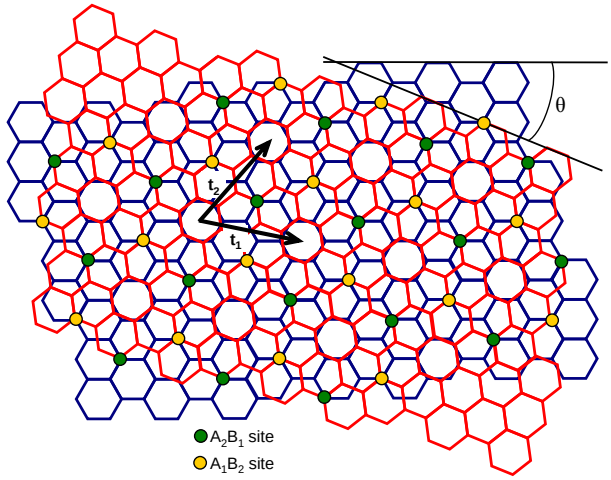

FIG. 2: (Color online) Sketch of the two turbostratic graphene layers under consideration. Both sheets are rotated with respect to each other with an angle $\theta \approx 21.787°$. t_1 and t_2 are the vectors of the Moiré unit cell.

IV. $K-K'$ COUPLINGS IN TURBOSTRATIC GRAPHENE LAYERS

Let us now suggest a heuristic argument to justify the use of our brane model for studying the graphene properties. A full demonstration of this statement is likely well beyond the scope of this paper but simple arguments suffice to be convinced by the analogy graphene bilayer/two-sheeted spacetime. In braneworld models, we have simply to consider the interaction between one fermion and domain walls described by a scalar field [24]. By contrast, a bilayer graphene is formally a many-body problem. Therefore we should normally consider the whole dynamics of carbon atoms and their electrons. This would be a very complicated task of course. Anyway, the existence of coupling terms proportional to g is straightforward for turbostratic graphene layers. When two graphene layers are twisted with respect to each other, a typical Moiré pattern can be observed [3–8] (Fig.2). This occurs when both layers are commensurate, i.e. when two specific kind of atoms of each layer can be superimposed periodically [3–8]. The Moiré pattern can be then described

through a periodic unit cell defined by vectors $\mathbf{t}_1$ and $\mathbf{t}_2$ (see Fig.2) and can only exist for a specific rotation angle $\theta = \theta_{p,q}$ (with $p, q \in \mathbb{N}$) between both layers.

Let us define $\mathbf{a}_1 = a_0(1/2, \sqrt{3}/2)$ and $\mathbf{a}_2 = a_0(-1/2, \sqrt{3}/2)$ the vectors of the real space which define the unit cell of the first graphene layer (see Fig.1a). a_0 is the lattice parameter. Two kinds of commensurate structures can be considered [3, 4]. The first one is such that the vectors of the Moiré unit cell are $\mathbf{t}_1 = p\mathbf{a}_1 + (p+q)\mathbf{a}_2$ and $\mathbf{t}_2 = -(p+q)\mathbf{a}_1 + (2p+q)\mathbf{a}_2$ such that $\gcd(q, 3) = 1$. The second case is such that $\mathbf{t}_1 = (p + q/3)\mathbf{a}_1 + (q/3)\mathbf{a}_2$ and $\mathbf{t}_2 = -(q/3)\mathbf{a}_1 + (p + 2q/3)\mathbf{a}_2$ with $\gcd(q, 3) = 3$. In both case, the rotation angle $\theta_{p,q}$ between both sheets is given by [3, 4]:

$$\cos\theta_{p,q} = \frac{3p^2 + 3pq + q^2/2}{3p^2 + 3pq + q^2} \tag{11}$$

In the first layer, the first K Dirac cone is located at $\mathbf{K} = (4\pi/(3a_0))(1, 0)$ while the K' Dirac cone is at $\mathbf{K}' = -\mathbf{K}$. By contrast, in the second layer, due to the rotation the K Dirac cone is located at $\mathbf{K}^\theta = (4\pi/(3a_0))(\cos\theta, \sin\theta)$ whenever the K' Dirac cone is at $\mathbf{K}^{\theta\prime} = -\mathbf{K}^\theta$ [3, 4]. Let $\mathbf{G}_1$ and $\mathbf{G}_2$ be the vectors of the unit cell of the reciprocal lattice of the Moiré pattern. Obviously, the Moiré pattern can be responsible for coupling between valleys of each layer [3–8]. Indeed, we get

$$\mathbf{G} = \mathbf{K} - \mathbf{K}^\theta = -(\mathbf{K}' - \mathbf{K}'^\theta) \tag{12}$$

for $K - K$ couplings, and

$$\mathbf{G}_c = \mathbf{K} - \mathbf{K}'^\theta = -(\mathbf{K}' - \mathbf{K}^\theta) \tag{13}$$

for $K - K'$ couplings. When $\gcd(q, 3) = 1$, then $\mathbf{G} = -(q/3)\,(2\mathbf{G}_1 + \mathbf{G}_2)$ and $\mathbf{G}_c = -(2p + q)\mathbf{G}_2$. While, when $\gcd(q, 3) = 3$, then $\mathbf{G} = -(q/3)\,(\mathbf{G}_1 + \mathbf{G}_2)$ and $\mathbf{G}_c = (1/3)(2p + q)\,(\mathbf{G}_1 - \mathbf{G}_2)$. The greater $\mathbf{G}$ and $\mathbf{G}_c$ are, the weaker the couplings are. As a consequence, one should consider the lowest values of p and q. A similar consideration leads us to expect that $K - K$ interlayer couplings are usually stronger than the $K - K'$ ones. Then, for the purposes of our study, it should be relevant to consider a structure which can suppress the $K - K$ couplings while enhancing the $K - K'$ interlayer couplings. We may consider for instance the case such that $\gcd(q, 3) = 1$ with $q = 1$. Indeed, in that case $\mathbf{G} = -(1/3)\,(2\mathbf{G}_1 + \mathbf{G}_2)$ is not a vector of the reciprocal lattice. By contrast $\mathbf{G}_c = -(2p + 1)\mathbf{G}_2$ is always a vector of the reciprocal lattice and is such that $G_c \approx 2K$ whatever p. The first relevant value to be considered is then $p = 1$. In this case, $\theta_{1,1} \approx 21.787°$ and we obtain the specific structure shown in Fig.2.

In a tight-binding approach it is possible to define the operator $a^\dagger_{\alpha(\beta),j}$ (respectively $a_{\alpha(\beta),j}$) which creates an electron (respectively a hole) on the site j of the sublattice "A" on the α graphene layer (or on the β graphene layer). The same convention is used for the sublattice "B". If one considers the interlayer coupling, one gets for the turbostratic system [3–9]:

$$H_c = -\sum_j t_{AB,j} a^\dagger_{\alpha,j} b_{\beta,j} - \sum_j t_{BA,j} b^\dagger_{\alpha,j} a_{\beta,j} + H.c. \tag{14}$$

where the energies $t_{uv,j}$ (with $u = A, B$ and $v = A, B$) are related to the interlayer hopping between the nearest sites of each layer. This dependence of $t_{uv,j}$ vs. the location j is very specific for two turbostratic graphene layers. In the structure considered here, we can see that no AA site exists by contrast to the AB sites (Fig.2). We then assume that $t_{AA,j} \approx t_{BB,j} \approx 0$. In addition, $t_{AB}(\mathbf{R}_j) = t_{AB,j} = -t'$ when $\mathbf{R}_j = (2/3)(\mathbf{t}_1 + \mathbf{t}_2) + (n\mathbf{t}_1 + m\mathbf{t}_2)$ (with $\mathbf{t}_1 = \mathbf{a}_1 + 2\mathbf{a}_2$ and $\mathbf{t}_2 = -2\mathbf{a}_1 + 3\mathbf{a}_2$) and $t_{BA}(\mathbf{R}_j) = t_{BA,j} = -t'$ when $\mathbf{R}_j = (1/3)(\mathbf{t}_1 + \mathbf{t}_2) + (n\mathbf{t}_1 + m\mathbf{t}_2)$, with $n, m \in \mathbb{N}$. $t_{AB,j}$ and $t_{BA,j}$ are equal to zero elsewhere. We use the following Fourier transform of the operators:

$$a_{\alpha(\beta)}(\mathbf{r}_j) = a_{\alpha(\beta),j} = \sum_k \frac{1}{\sqrt{N}} a_{\alpha(\beta),\mathbf{q}_k} e^{i\mathbf{r}_j \cdot \mathbf{q}_k^{\alpha(\beta)}} \tag{15}$$

with a similar convention for $b_{\alpha(\beta),j}$ and $t_{uv,j}$. $\mathbf{q}_k^{\alpha(\beta)}$ are vectors of the reciprocal lattice of graphene sheet α (or β). Let us consider a single particle state with momentum $\mathbf{k}$ such that we can consider the restricted Fourier representation of the Hamiltonian: $H_c = H_{c,\mathbf{K}+\mathbf{k}} + H_{c,\mathbf{K}'+\mathbf{k}} + H_{c,\mathbf{K}^\theta+\mathbf{k}} + H_{c,\mathbf{K}^{\theta\prime}+\mathbf{k}}$ such that $H_c = \Psi^\dagger \mathcal{H}_c \Psi$ with

$$\mathcal{H}_c = -t'\sigma_1 \otimes \gamma^5 \tag{16}$$

and

$$\begin{aligned}\Psi^t &= \left(a_{\alpha,K} \;\; b_{\alpha,K} \;\; a_{\alpha,K'} \;\; b_{\alpha,K'} \;\; a_{\beta,K} \;\; b_{\beta,K} \;\; a_{\beta,K'} \;\; b_{\beta,K'} \right) \\ &\sim \left(\psi^t_\alpha \;\; \psi^t_\beta \right)\end{aligned} \tag{17}$$

Using the above notations, and after a convenient SU(2) rotation such that $b \to ib$, the Lagrangian term related to $\mathcal{H}_c$ in Dirac notation becomes $\mathcal{L}_c = \overline{\Psi} i\Gamma^5 D_5 \Psi$, i.e. Eq. (8) related to Eq. (7).

Now, the coupling constant g can be then defined as $g = t'/\hbar v_F$ and the phenomenological distance is $\delta = \hbar v_F/t'$. Basically, g and δ must depend on the real distance d between each graphene sheet. Indeed, the hooping energy t' varies as [8]: $t' \sim t_0 \exp(5.43 \cdot (1 - d/a_{\rm m}))$, with $t_0 \approx 0.3$ eV [2, 8, 9], and here d is the distance between two layers, while $a_{\rm m}$ is the nearest interlayer distance, $a_{\rm m} = 3.35$ Å. For closest layers ($d = a_{\rm m}$), we get δ of about 22 Å (i.e. $g \approx 4.5 \cdot 10^8$ m^{-1}). As an indication, note that for $d = 2a_{\rm m}$ (respectively $d = 5a_{\rm m}$), one gets $g \approx 2 \cdot 10^6$ m^{-1} (respectively $g \approx 1.7 \cdot 10^{-1}$ m^{-1}).

V. PHENOMENOLOGY OF THE MODEL

Following previous works [24–26], we focus on the non-relativistic limit of our Dirac like equation. Defining $\nabla = (\partial_1, \partial_2)$, $\mathbf{A} = (A_1, A_2)$, $\sigma = (\sigma_1, \sigma_2)$ and $B_3 = \partial_1 A_2 - \partial_2 A_1$ and using: $F_{A(B)} = \begin{pmatrix} \chi_{A(B)} \\ \theta_{A(B)} \end{pmatrix}$,and following the well-known standard procedure, a two-layer Pauli equation can be derived from Eq. (10) [24–27]:

$$i\hbar\frac{\partial}{\partial t}\begin{pmatrix} F_{A,\alpha} \\ F_{A,\beta} \end{pmatrix} = \{\mathbf{H}_0 + \mathbf{H}_{cm}\}\begin{pmatrix} F_{A,\alpha} \\ F_{A,\beta} \end{pmatrix} \quad (18)$$

where $F_{A,\alpha}$ and $F_{A,\beta}$ correspond to the wave functions in the graphene layers α and β respectively. The Hamiltonian $\mathbf{H}_0$ is a block-diagonal matrix such that $\mathbf{H}_0$ =diag($\mathbf{H}_\alpha, \mathbf{H}_\beta$), where each block is simply the effective Pauli Hamiltonian expressed in each graphene layer [24–27]:

$$\mathbf{H}_{\alpha(\beta)} = -\frac{\hbar^2}{2m}\left(\nabla - i\frac{q}{\hbar}\mathbf{A}_{\alpha(\beta)}\right)^2 + \mu_3 B_{3,\alpha(\beta)} + V_{\alpha(\beta)} \quad (19)$$

such that $\mathbf{A}_\alpha$ and $\mathbf{A}_\beta$ correspond to the magnetic vector potentials on the layers α and β respectively. The same convention is applied to the magnetic fields $\mathbf{B}_{\alpha(\beta)}$ and to the potentials $V_{\alpha(\beta)}$. In the following, since we consider neutral excitons, we can set $V_{\alpha(\beta)} = 0$. In addition, we will show hereafter that $B_{3,\alpha(\beta)} = 0$ in the device under consideration (see section VI). We set $\mu = \gamma(\hbar/2)\sigma$ where γ is the pseudo-gyromagnetic ratio and μ the pseudo-magnetic moment related to the pseudo-spin of the particle [22]. With this choice, the present approach can be extended to any particle endowed with a magnetic moment whatever its spin value.

In addition to these usual terms, the two-layer graphene Hamiltonian comprises also a new specific term [24–27]:

$$\mathbf{H}_{cm} = \begin{pmatrix} 0 & -ig\boldsymbol{\mu}\cdot\{\mathbf{A}_\alpha - \mathbf{A}_\beta\} \\ ig\boldsymbol{\mu}\cdot\{\mathbf{A}_\alpha - \mathbf{A}_\beta\} & 0 \end{pmatrix} \quad (20)$$

$\mathbf{H}_{cm}$ is obviously not conventional and describes the coupling of the layers through electromagnetic fields. It vanishes for null magnetic vector potentials. Intuitively, the coupling generated by this term will imply Rabi oscillations of electrons or holes between both graphene sheets due to electronic delocalization.

VI. EXCITON SWAPPING BETWEEN TWO GRAPHENE LAYERS AND EXPERIMENTAL DEVICE

Guided by the previous equations, we now suggest an experimental approach for testing exciton swapping between two graphene layers. An incident electromagnetic wave with a convenient energy can excite an electron-hole bound pair (i.e. an exciton) [17–21] on a first graphene layer (G_α). In the best of our knowledge, studies related to the magnetic moment of exciton in graphene are still lacking. Nevertheless, exciton should exhibit resonance states endowed with non-zero magnetic moment μ [30] due to the combination of the electron/hole magnetic moments [22], possibly supplemented by an orbital magnetic moment. One can then expect to induce a coupling through $\mathbf{H}_{cm}$ between G_α and a second graphene layer G_β leading to a swapping of the exciton from G_α towards G_β. Afterwards, the exciton decay on the second layer could be recorded.

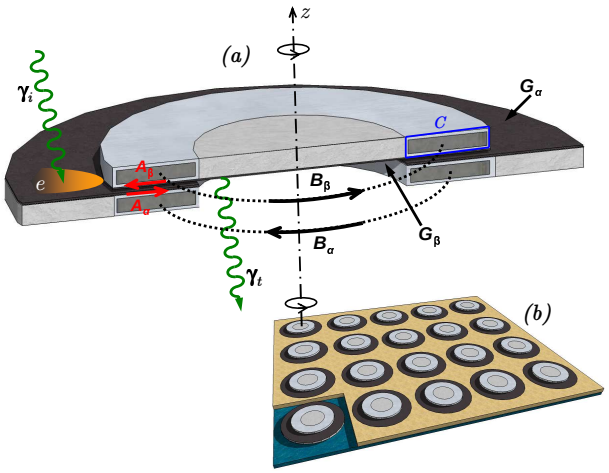

FIG. 3: (Color online). Sketch of a feasible experimental setup. (a): Basic setup. Two coaxial annular magnets, with different inner and outer diameters, covered by an insulating material. The upper ring is filled up with an opaque material. Two magnetic fields (B_α and B_β) turn around the symmetry axis of the magnets and are opposite. Two graphene layers (G_α and G_β) are considered, each one deposited on a face of a magnet. The geometry of the device allows the existence of two opposite magnetic vector potentials (A_α and A_β), each one in the vicinity of a graphene layer. An incident photon γ_i pumps an exciton e on G_α. A photon γ_t resulting from the exciton decay on G_β can be recorded. (b): Full setup. Rectangular array of annular devices deposited on a transparent substrate (blue layer). The area between the toroidal magnets is filled with an opaque material (yellowish layer). Such a setup allows to enhance the recorded signal by increasing the graphene area.

The required magnetic vector potentials can be produced with the following device. Let us consider two coaxial annular magnets covered by an insulating material (see Fig.3a). Both magnets have the same rectangular section. Both magnetic fields ($\mathbf{B}_\alpha$ and $\mathbf{B}_\beta$) inside the magnets turn around the symmetry axis of the magnets and are opposite. $B_\alpha = B_\beta = 0$ outside the magnets due to the toroidal topology [31]. Only a magnetic vector potential $\mathbf{A}$ exists outside the magnet [31] (i.e. $\nabla \times \mathbf{A} = 0$). Boundary conditions result from $\oint_C \mathbf{A}\cdot d\mathbf{l} = \Phi$, where C is a contour on a magnet (see

Fig.3) and Φ the magnetic flux inside a magnet. The geometry of the device leads to two opposite magnetic vector potentials ($\mathbf{A}_\alpha$ and $\mathbf{A}_\beta$), each one in the vicinity of a graphene layer (G_α and G_β) deposited on a face of a magnet (see Fig.3a). A straightforward calculation shows that $|\mathbf{A}_\alpha - \mathbf{A}_\beta| \sim 2A_0 d/(L+l)$, with d the distance between the two layers, L and l are the length and width of rectangular section of the magnets. If one considers a superconducting magnet, then $A_0 \sim nh/(4e(L+l))$, where n is an integer (h is the Planck constant and e the electric charge), due to the magnetic flux quantization [32]. For instance, if $L = 1$ μm and $l = 10$ nm [31] and with $d = 2a_{\rm m}$, one gets $|\mathbf{A}_\alpha - \mathbf{A}_\beta| \approx 1.4 \cdot 10^{-12}$ T·m for $n = 1$.

The insulating material is the substrate on which the graphene layers are deposited. This allows a gated graphene leading to electron and hole that share the same effective mass [16]. The efficient graphene area can be increased by using a large array of micro-annular devices (see Fig.3b).

The excitonic swapping can be described as follows. One looks for an exciton wave function in the form:

$$\begin{aligned} |\Phi(t)\rangle &= \begin{pmatrix} F_{A,\alpha}(t) \\ F_{A,\beta}(t) \end{pmatrix} \\ &= a_\alpha(t) \begin{pmatrix} \Psi_s \\ 0 \end{pmatrix} + a_\beta(t) \begin{pmatrix} 0 \\ \Psi_s \end{pmatrix} \end{aligned} \tag{21}$$

where it is assumed that $\boldsymbol{\mu}\Psi_s = \pm\mu\Psi_s$, i.e. Ψ_s is an eigenstate of $\boldsymbol{\mu}$ with an eigenvalue μ different from zero. For an exciton, the lowest expected value can be estimated by $\mu \sim e\hbar/m$ [30], i.e. $\mu \approx 3.5 \cdot 10^{-22}$ J·T^{-1} for an effective electron/hole mass about 0.3 eV [16]. Putting Eq. (21) into the Pauli equation (18) leads to the following system of coupled differential equations:

$$\frac{d}{dt}a_\alpha = -\kappa a_\beta - (1/2)\Gamma_0 a_\alpha + \delta(t - t_i) \tag{22}$$

and

$$\frac{d}{dt}a_\beta = \kappa a_\alpha - (1/2)\Gamma_0 a_\beta \tag{23}$$

with $\kappa = \mu g\,(A_\alpha - A_\beta)/\hbar$. With the above mentioned values, one can roughly estimate $\kappa \approx 2.1 \cdot 10^9$ rad·s^{-1}. Γ_0 is the exciton decay rate conveniently introduced in the equations in agreement with the lifetime τ of the exciton ($\Gamma_0 = \tau^{-1}$). We assume that τ is included between 10 fs and 200 ps [21, 33] ($5{\cdot}10^9$ s$^{-1} \leq \Gamma_0 \leq 10^{14}$ s^{-1}). $\delta(t - t_i)$ is a Dirac delta source such that the exciton is created at $t = t_i$ in the layer α. Then, $a_\alpha(t = t_i) = 1$ and $a_\beta(t = t_i) = 0$. The number of excitons is then given by $\mathcal{N}_\alpha = \sum_i a_\alpha^* a_\alpha$ (respectively $\mathcal{N}_\beta = \sum_i a_\beta^* a_\beta$) in layer α (respectively in layer β). In the continuous limit such that $\mathcal{M}$ excitons are produced per second, from Eqs. (22) and (23), one easily obtains three Bloch-like equations:

$$\frac{d}{dt}\mathcal{N}_\alpha = -\kappa\mathcal{U} - \Gamma_0\mathcal{N}_\alpha + \mathcal{M} \tag{24}$$

and

$$\frac{d}{dt}\mathcal{N}_\beta = \kappa\mathcal{U} - \Gamma_0\mathcal{N}_\beta \tag{25}$$

and

$$\frac{d}{dt}\mathcal{U} = 2\kappa\mathcal{N}_\alpha - 2\kappa\mathcal{N}_\beta - \Gamma_0\mathcal{U} \tag{26}$$

with $\mathcal{U} = \sum_i (a_\alpha^* a_\beta + a_\alpha a_\beta^*)$. Since layer α is continuously supplied with new excitons thanks to an incident photon flux $\mathcal{I}_0$, the exciton source is such that $\mathcal{M} = \rho_{\rm eff}\mathcal{I}_0$. $\rho_{\rm eff}$ is the photon-to-exciton conversion efficiency. Eqs. (24) to (26) must present short-time transient solutions due to $-\Gamma_0\mathcal{N}_{\alpha(\beta)}$ and $-\Gamma_0\mathcal{U}$ terms. As a consequence, we look for stationary solutions such that $d\mathcal{N}_\alpha/dt = d\mathcal{N}_\beta/dt = d\mathcal{U}/dt = 0$. Eqs. (24) to (26) can be then trivially solved. The number of excitons in each graphene layers are:

$$\mathcal{N}_\alpha = \frac{2\kappa^2 + \Gamma_0^2}{\Gamma_0\,(4\kappa^2 + \Gamma_0^2)}\mathcal{M}, \text{ and } \mathcal{N}_\beta = \frac{2\kappa^2}{\Gamma_0\,(4\kappa^2 + \Gamma_0^2)}\mathcal{M} \tag{27}$$

and the number of new created excitons balances the number of decaying excitons, i.e. $\mathcal{M} = \Gamma_0\,(\mathcal{N}_\alpha + \mathcal{N}_\beta)$. Note that in the present approach, we do not consider any saturation effect regarding to the number of excitons per unit area. Then for a fixed area, $\mathcal{N}_\alpha + \mathcal{N}_\beta$ should be limited and $\mathcal{M}/\Gamma_0$ likewise. As a consequence, for a given value of $\mathcal{M}$, the present approach is not valid when $\Gamma_0 \to 0$.

The photon flux $\mathcal{I}_t$ emitted from the second graphene layer β is $\mathcal{I}_t = n\Gamma_0\mathcal{N}_\beta$ where n is the number of photons that results from the exciton decay. The effective optical transmission coefficient $\mathcal{T}$ of the device is $\mathcal{T} = \mathcal{I}_t/\mathcal{I}_0$, and one gets:

$$\mathcal{T} = n\rho_{\rm eff}\frac{2\kappa^2}{4\kappa^2 + \Gamma_0^2} \tag{28}$$

The excitons transferred from layer α to layer β are then detected through recorded photons due to excitonic decay (see Fig.3a). Let us consider the simplest process such that $n\rho_{\rm eff} = 1$, i.e. every exciton decays into a single photon, and each photon creates a single exciton [34]. With the above values, the best expected transmission $\mathcal{T}$ could reach 21 %, which is of course a fair value in an experimental context.

VII. CONCLUSIONS

Using a theoretical approach previously considered to describe a Universe made of two braneworlds [24–27], we have proposed a new theoretical description of the phenomenology of two turbostratic graphene sheets. This suggests a new way to describe multilayer graphene, which will deserve further studies. We have shown that the transfer of excitons between the two graphene sheets is allowed for some specific electromagnetic conditions.

While the excitons are produced by incident light on the first graphene layer, photons could be recorded in front of the second graphene layer where the swapped exciton decays. Such a system is a solid-state realization of a two-brane Universe, for which it has been shown that matter swapping between two braneworlds could occur [24–27]. As a consequence, any experimental evidence of this effect in graphene bilayers would be relevant in the outlook of braneworld studies. Since the magnetic fields inside the magnets can be controlled with a transient external magnetic field, it is possible to turn on or off the device. We can then expect to get a new kind of electro-optic light modulator with hysteresis.

Acknowledgements

The authors are grateful to Philippe Lambin, Luc Henrard and Nicolas Reckinger for useful discussions and comments.

[1] K.S. Novoselov, A.K. Geim, S.V. Morozov, D. Jiang, M.I. Katsnelson, I.V. Grigorieva, S.V. Dubonos, A.A. Firsov, Nature **438** (2005) 197, arXiv:cond-mat/0509330 [cond-mat.mes-hall].

[2] A.H. Castro Neto, F. Guinea, N.M.R. Peres, K.S. Novoselov, A.K. Geim, Rev. Mod. Phys. **81** (2009) 109, arXiv:0709.1163 [cond-mat.other].

[3] J.M.B. Lopes dos Santos, N.M.R. Peres, A.H. Castro Neto, Phys. Rev. Lett. **99** (2007) 256802, arXiv:0704.2128 [cond-mat.mtrl-sci];
J.M.B. Lopes dos Santos, N.M.R. Peres, A.H. Castro Neto, arXiv:1202.1088 [cond-mat.mtrl-sci].

[4] S. Shallcross, S. Sharma, E. Kandelaki, O.A. Pankratov, Phys. Rev. B **81** (2010) 165105, arXiv:0910.5811 [cond-mat.mtrl-sci].

[5] R. Bistritzer, A.H. MacDonald, Phys. Rev. B **81** (2010) 245412, arXiv:1002.2983 [cond-mat.mes-hall].

[6] E.J. Mele, Phys. Rev. B **81** (2010) 161405(R), arXiv:1001.5190 [cond-mat.mes-hall].

[7] R. Bistritzer, A.H. MacDonald, PNAS **108** (2011) 12233, arXiv:1009.4203 [cond-mat.mes-hall].

[8] G. Trambly de Laissardière, D. Mayou, L. Magaud, Nano Lett. **10** (2010) 804.

[9] E.V. Castro, K.S. Novoselov, S.V. Morozov, N.M.R. Peres, J.M.B. Lopes dos Santos, J. Nilsson, F. Guinea, A.K. Geim, A.H. Castro Neto, J. Phys.: Condens. Matter **22**, 175503 (2010), arXiv:0807.3348 [cond-mat.mes-hall].

[10] M. Mecklenburg, B.C. Regan, Phys. Rev. Lett. **106** (2011) 11680, arXiv:1003.3715 [cond-mat.mes-hall].

[11] M.I. Katsnelson, K.S. Novoselov, Solid State Commun. **143** (2007) 3, arXiv:cond-mat/0703374 [cond-mat.mes-hall].

[12] F. de Juan, A.G. Grushin, M.A.H. Vozmediano, Phys. Rev. B **82** (2010) 125409, arXiv:1002.3111 [cond-mat.str-el].

[13] M.I. Katsnelson, K.S. Novoselov, A.K. Geim, Nature Phys. **2** (2006) 620, arXiv:cond-mat/0604323 [cond-mat.mes-hall].

[14] F.D.M. Haldane, Phys. Rev. Lett. **61** (1988) 2015.

[15] G.W. Semenoff, Phys. Rev. Lett. **53** (1984) 2449.

[16] S.Y. Zhou, D.A. Siegel, A.V. Fedorov, F. El Gabaly, A. K. Schmid, A.H. Castro Neto, A. Lanzara, Nature Mat. **7** (2008) 259, arXiv:0804.1818 [cond-mat.mtrl-sci];
S.Y. Zhou , G.H. Gweon , A.V. Federov , P.N. First , W.A. De Heer , D.H. Lee , F. Guinea , A.H.C. Neto , A. Lanzara , Nature Mat. **6** (2007) 770, arXiv:0709.1706v2 [cond-mat.mtrl-sci].

[17] R. Dillenschneider, J.H. Han, Phys. Rev. B **78** (2008) 045401, arXiv:0709.1230 [cond-mat.str-el].

[18] I. Santoso, P.K. Gogoi, H.B. Su, H. Huang, Y. Lu, D. Qi, W. Chen, M.A. Majidi, Y.P. Feng, A.T.S. Wee, K.P. Loh, T. Venkatesan, R.P. Saichu, A. Goos, A. Kotlov, M. Rübhausen, A. Rusydi, Phys. Rev. B **84** (2011) 081403 (R), arXiv:1101.3060 [cond-mat.str-el].

[19] A. Bostwick, T. Ohta, T.Seyller, K. Horn, E. Rotenberg, Nature Physics **3** (2007) 36.

[20] N.M.R. Peres, R.M. Ribeiro, A.H. Castro Neto, Phys. Rev. Lett. **105** (2010) 055501, arXiv:1002.0464 [cond-mat.mes-hall].

[21] L. Yang, Phys. Rev. B **83** (2011) 085405.

[22] D. Xiao, W. Yao, Q. Niu, Phys. Rev. Lett. **99**, 236809 (2007).

[23] V.A. Rubakov, M.E. Shaposhnikov, Phys. Lett. **125B**, 136 (1983);
A. Lukas, B.A. Ovrut, K.S. Stelle, D. Waldram, Phys. Rev. D **59**, 086001 (1999), arXiv:hep-th/9803235;
R. Davies, D.P. George, R.R. Volkas, Phys. Rev. D **77**, 124038 (2008), arXiv:0705.1584 [hep-ph];
Y.-X. Liu, L.-D. Zhang, L.-J. Zhang, Y.-S. Duan, Phys. Rev. D **78**, 065025 (2008), arXiv:0804.4553 [hep-th].

[24] M. Sarrazin, F. Petit, Phys. Rev. D **81**, 035014 (2010), arXiv:0903.2498 [hep-th].

[25] F. Petit, M. Sarrazin, Phys. Lett. B **612** (2005) 105 , arXiv:hep-th/0409084.

[26] M. Sarrazin, F. Petit, Int. J. Mod. Phys. A **22** (2007) 2629, arXiv:hep-th/0603194.

[27] M. Sarrazin, G. Pignol, F. Petit, V.V. Nesvizhevsky, Phys. Lett. B **712** (2012) 213, arXiv:1201.3949 [hep-ph].

[28] A. Connes, J. Lott, Nucl. Phys. **18**B (Proc. Suppl.) (1991) 29;
A. Connes, *Non-Commutative Geometry* (Academic Press, San Diego, CA, 1994).

[29] N.A. Viet, K.C. Wali, Phys. Rev. D **67** (2003) 124029, hep-th/0212062;
N.A. Viet, K.C. Wali, Int. J. Mod. Phys. A **11** (1996) 533, hep-th/9412220.

[30] L.C. Smith, J.J. Davies, D. Wolverson, H. Boukari, H. Mariette, V.P. Kochereshko, R.T. Phillips, Phys. Rev. B **83**, 155206 (2011);
J.J. Davies, D. Wolverson, V.P. Kochereshko, A.V. Platonov, A.F. Ioffe, R.T. Cox, J. Cibert, H. Mariette, C. Bodin, C. Gourgon, E.V. Ubyivovk, Yu. P. Efimov, S.A. Eliseev, Phys. Rev. Lett. **97**, 187403 (2006).

[31] A. Tonomura, T. Matsuda, B. Suzuki, A. Fukuhara, N.

Osakabe, H. Umezaki, J. Endo, K. Shinagawa, Y. Sugita, H. Fujiwara, Phys. Rev. Lett. **48** (1982) 1443;
A. Tonomura, H. Umezaki, T. Matsuda, N. Osakabe, J. Endo, Y. Sugita, Phys. Rev. Lett. **51** (1983) 331.

[32] H. Doll, M. Näbauer, Phys. Rev. Lett. **7** (1961) 51.

[33] V. Perebeinos, J. Tersoff, P. Avouris, Nano Lett. **5** (2005) 2495;
C.D. Spataru, S. Ismail-Beigi, R.B. Capaz, and S.G. Louie, Phys. Rev. Lett. **95**, 247402 (2005).

[34] S. Albrecht, S. Schäfer, I. Lange, S. Yilmaz, I. Dumsch, S. Allard, U. Scherf, A. Hertwig, Dieter Neher, Org. Electron. **13** (2012) 615622;
V.I. Klimov, J. Phys. Chem. B **110** (2006) 16827.